J. Chem. Thermodynamics **1996,** 28, 1153–1164

JCT

Critical parameters of $\{xCO_2 + (1 - x)CHF_3\}$ for $x = (1.0000, 0.7496, 0.5013, \text{and } 0.2522)$

Y. Suehiro,[a] M. Nakajima, K. Yamada, and M. Uematsu

Department of Mechanical Engineering, Keio University, Yokohama 223, Japan

The (p, ρ, T) measurements and visual observations of the meniscus for $\{xCO_2 + (1 - x)CHF_3\}$ with $x = (1.0000, 0.7496, 0.5013, \text{and } 0.2522)$ were carried out carefully in the critical region by a metal-bellows volumometer with optical cell. The critical properties of T_c, ρ_c, and p_c measured for pure CO_2 were compared with values given in the literature and the results confirmed the capability of the apparatus. The critical parameters of T_c, ρ_c, and p_c for the mixtures measured, based on the results for observation of the critical opalescence, are presented. The composition dependence of these critical properties is compared with that predicted by cubic equations of state.

1. Introduction

The critical parameters of the mixtures are the key properties for innovation in supercritical fluid technology. An apparatus has been developed for measuring with high accuracy the vapour–liquid critical parameters of fluids and fluid mixtures of known composition. In this paper, the apparatus is described and experimental results are given of the critical parameters of T_c, ρ_c, and p_c for pure CO_2 and $\{xCO_2 + (1 - x)CHF_3\}$ with $x = (0.7496, 0.5013, \text{and } 0.2522)$. The measurements for pure CO_2 have been carried out to illustrate the capability of the apparatus. The critical parameters for the mixtures are illustrated as a function of composition, and the comparison with the values predicted by cubic equations of state is reported.

2. Apparatus and experimental

The apparatus used was designed and constructed for measuring the vapour–liquid critical properties of fluids and fluid mixtures of a fixed composition in the temperature range from $T = 250$ K to $T = 500$ K at pressures up to $p = 100$ MPa. The main part of the apparatus was a volumometer, shown in figure 1, in which the sample to be measured was loaded. The entire apparatus is shown schematically in figure 2.

[a] To whom correspondence should be addressed.

0021–9614/96/101153 + 12 $18.00/0

The volumometer consisted of an optical cell and metal bellows in a pressure vessel made of a stainless steel (SUS 630). Through the window in the optical cell of 8 mm diameter, the meniscus at the vapour–liquid interface of the sample was observed by a CCD camera. The pictures were monitored on a display and recorded by a video tape recorder. The windows made of synthetic sapphire, whose dimensions were 12 mm in thickness and 22 mm in diameter, were set on two sides of the optical cell. The height of the space where the sample was loaded in the volumometer was designed to be as small as possible. The metal bellows made of a (nickel + chromium) alloy (Inconel 718) were designed with reference to previous experience.[1, 2] Dimensions of the bellows with 50 corrugations were: 70 mm long, 0.12 mm thick, 22 mm o.d., 8 mm i.d., and 1.77 cm^2 in effective cross-sectional area. A rod with a magnetic core was attached to the closure of the bellows. The rod travelled inside the pressure tubing, and the position of the magnetic core was detected by a linear variable differential transformer mounted on a linear stage. The displacement of the stage was measured by a digital indicator with a resolution of $\pm 0.5\ \mu m$. Nitrogen gas was supplied to the outside of the bellows in the pressure vessel from the pressure-measurement system and pressurized with a pressure intensifier using a hand pump. By increasing or reducing the pressure of the nitrogen gas, the bellows were compressed or expanded. The inner volume V_i of the volumometer and its variation with the bellows displacement were calibrated from the known density of water with an uncertainty of $\pm 5{\cdot}10^{-4}{\cdot}V_i$. Thus, V_i changed from about 18 cm^3 to 12 cm^3 by compressing the bellows a distance of 30 mm. The whole volume V_0 of the (volumometer + connecting lines + supply vessel) was calibrated in the same manner as V_i with an uncertainty of $\pm 5{\cdot}10^{-4}{\cdot}V_0$. In the body of the pressure vessel, a well was drilled for inserting a platinum resistance thermometer.

The volumometer was immersed in a thermostatted oil bath with windows on two sides. The bath, equipped with two independent electric heaters and one cooler, was filled with silicone oil as a heat-transfer medium, which was circulated by two

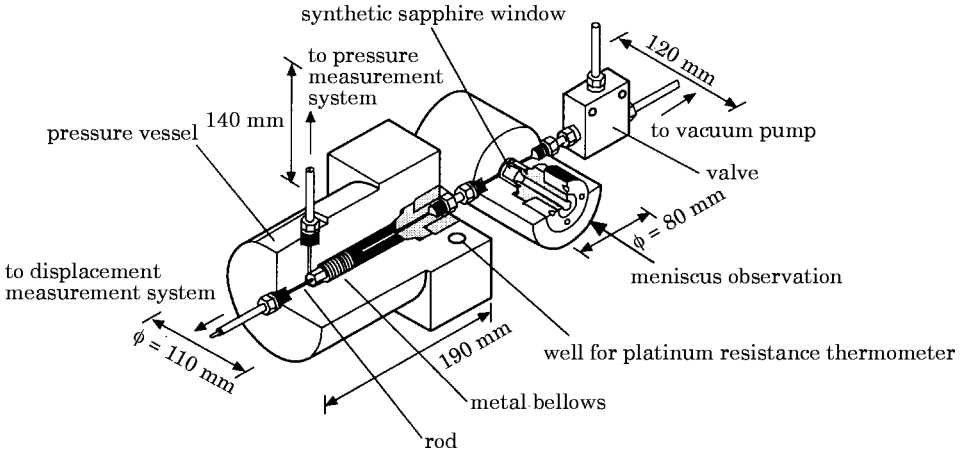

FIGURE 1. The volumometer with the optical cell.

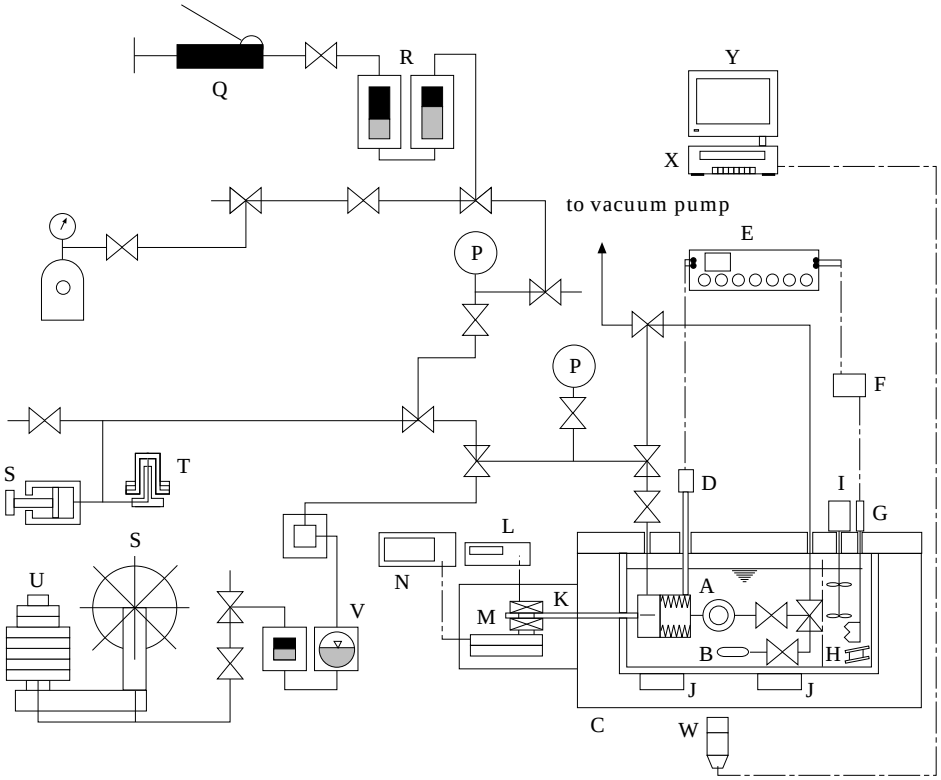

FIGURE 2. Schematic diagram of the experimental apparatus. A, volumometer with the optical cell; B, supply vessel; C, thermostatted oil bath; D, platinum resistance thermometer; E, thermometer bridge; F, P.I.D. controller; G, heater (1.2 kW + 0.3 kW); H, cooler (0.3 kW); I, stirrer; J, six heaters (0.275 kW); K, linear variable differential transformer; L, digital multimeter; M, linear stage; N, digital indicator; O, N_2 bottle; P, Bourdon gauge; Q, hand pump; R, pressure intensifier; S, pressure controller; T, air-piston pressure gauge (0.8 MPa to 20.8 MPa); U, oil-operated dead-weight pressure gauge (20.8 MPa to 100 MPa); V, N_2-to-Hg-to-oil separator; W, CCD camera; X, video tape recorder; Y, display.

stirrers. One 1.2 kW heater was used as a base load for $T > 305$ K, and the electric power supplied to the other heater with a capacity of 0.3 kW was controlled by a P.I.D. controller. The cooler was used as a base load for $T < 305$ K. Evacuated thermal insulation 20 mm thick was also provided around the bath except on its upper side. Six electric heaters were set on the outside of the insulation to offset heat losses from the bath. The temperature detected at the well drilled in the body of the volumometer was set at the desired value within ± 0.1 mK and was kept constant to within ± 20 mK for $T < 305$ K, and within ± 3 mK for $T > 305$ K during the measurements at a given temperature. A 25 Ω platinum resistance thermometer (Chino: Model R 800-2) was inserted in the well and the temperature measured with the aid of this thermometer by a thermometer bridge (Tinsley: Type 5840). The thermometer was calibrated with a precision of

TABLE 1. Experimental results for the (p, ρ, T) properties and observations of the meniscus for CO_2, where T is the temperature (ITS-90), ρ the density, and p the pressure

T/K	ρ/(kg·m^{-3})	p/MPa	Number of phases	Observation[a]
303.920	460.72	7.3414	2	N
303.940	460.80	7.3445	2	N
303.950	467.85	7.3461	2	N
303.960	460.82	7.3479	2	N
303.980	462.43	7.3513	2	N
303.980	468.02	7.3515	2	N
304.000	467.91	7.3550	2	N
304.020	468.04	7.3583	2	L
304.040	468.05	7.3617	2	L
304.050	467.84	7.3633	2	L
304.060	468.00	7.3646	2	L
304.080	468.00	7.3680	2	L
304.100	467.88	7.3720	2	L
304.100	467.98	7.3715	2	L
304.120	467.90	7.3755	2	L
304.120	468.00	7.3747	2	L
304.120	468.18	7.3753	2	L
304.140	465.92	7.3789	2	L
304.140	467.90	7.3795	2	L
304.140	467.99	7.3781	2	L
304.160	463.64	7.3825	2	L
304.160	467.89	7.3824	2	L
304.160	468.13	7.3816	2	L
304.180	462.20	7.3854	1	D
304.180	466.08	7.3845	1	D
304.180	467.11	7.3846	1	D
304.180	467.49	7.3850	1	D
304.180	467.76	7.3858	1	D
304.180	467.98	7.3845	1	D
304.180	468.00	7.3851	1	D
304.180	468.49	7.3844	1	D
304.180	469.00	7.3845	1	D
304.180	470.05	7.3843	1	D
304.185	467.05	7.3855	1	D
304.185	467.49	7.3855	1	D
304.185	468.00	7.3857	1	D
304.185	468.04	7.3856	1	D
304.185	468.99	7.3857	1	D
304.185	470.05	7.3854	1	D
304.190	468.02	7.3864	1	O
304.190	470.03	7.3861	1	O
304.195	468.02	7.3876	1	O
304.200	466.39	7.3889	1	O
304.200	467.58	7.3889	1	O
304.200	468.04	7.3885	1	O
304.200	470.00	7.3880	1	O
304.210	467.99	7.3899	1	L
304.220	466.67	7.3924	1	L
304.240	466.49	7.3956	1	L

[a] Observations are classified into the following four groups according to the intensity of the critical opalescence: N, no opalescence; L, light opalescence; O, opalescence; D, dark opalescence.

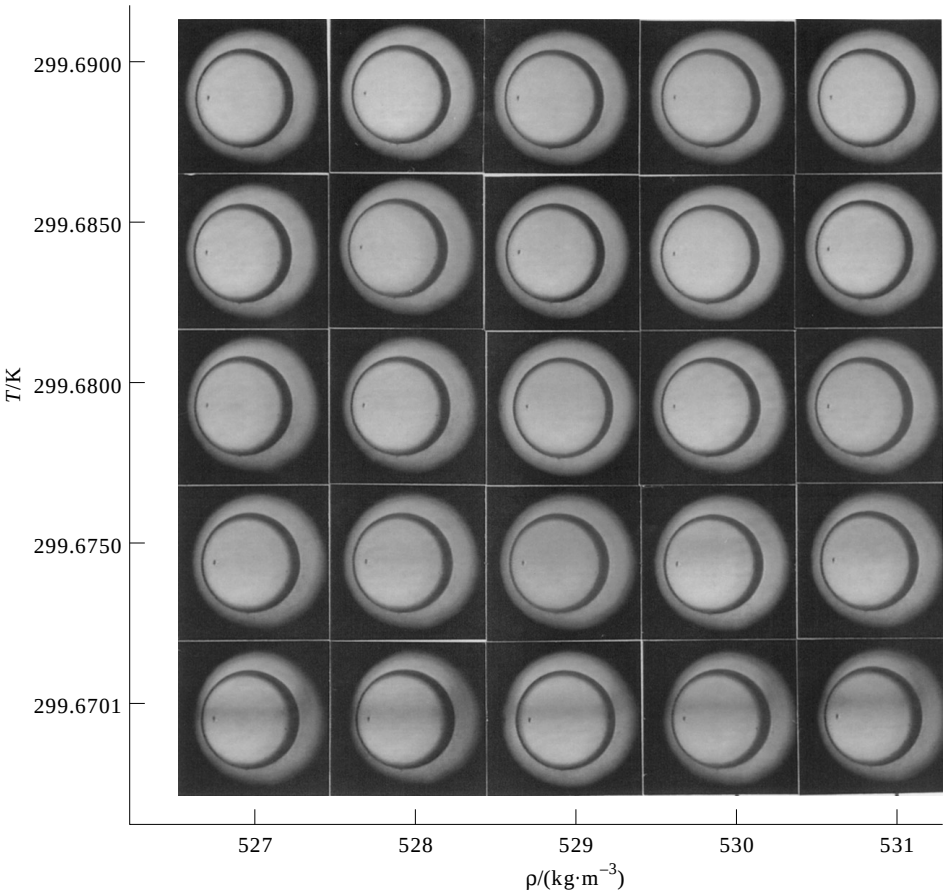

FIGURE 3. The results for observation of the critical opalescence of $\{xCO_2 + (1 - x)CHF_3\}$ with $x = 0.2522$.

± 1 mK on IPTS-68 at the National Research Laboratory of Metrology, Tsukuba, Japan, and its calibration results were converted to ITS-90. The resistance of the thermometer at the triple-point temperature of water was measured periodically.

TABLE 2. Experimental results for the critical parameters for $\{xCO_2 + (1 - x)CHF_3\}$, where T_c is the critical temperature (ITS-90), ρ_c the critical density, and p_c the critical pressure

x	T_c/K	ρ_c/(kg·m^{-3})	p_c/MPa
1.0000	304.18 ± 0.02	468 ± 1	7.38 ± 0.01
0.7496	301.75 ± 0.02	506 ± 1	6.67 ± 0.01
0.5013	300.50 ± 0.02	521 ± 10	6.03 ± 0.01
0.2522	299.675 ± 0.010	528.9 ± 1.0	5.401 ± 0.002

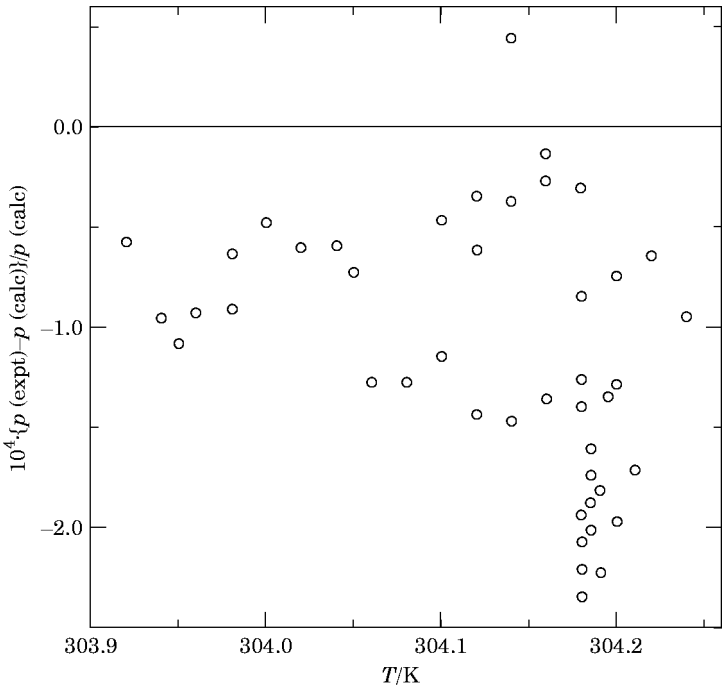

FIGURE 4. Deviation plots of the vapour pressure for pure CO_2 from a correlation by Duschek *et al*.[3]

The pressure of the nitrogen gas was measured with two different pressure gauges, depending on the pressure range: an air-piston pressure gauge (Ruska: Model 2470-701) for $0.8\ \text{MPa} < p \leq 20.8\ \text{MPa}$ with a precision of $\pm 1 \cdot 10^{-4} \cdot p$, and an oil-operated dead-weight pressure gauge (Tokyo Keiki: Model SH2) for $20.8\ \text{MPa} < p \leq 100\ \text{MPa}$ with a precision of $\pm 3 \cdot 10^{-4} \cdot p$. These pressure gauges were also used for generating a constant pressure. The pressure of the sample was set at the desired value within a tenth of the uncertainty in the pressure measurements. Even if the bellows were held in balance, the pressure of the sample confined in the bellows was different from that exerted by the nitrogen gas on the bellows. The pressure difference was about 0.24 MPa at the state where the bellows were compressed by 30 mm, and it was calibrated within ± 1 kPa as a function of the bellows displacement and temperature.

Each component to be mixed was weighed separately with a precision chemical balance (Chyo: Model C_2-3000) with an uncertainty of ± 2 mg. The sample was then prepared in a supply vessel (volume: 52 cm^3) into which each pure component was charged separately by condensation. The mass fraction w was adjusted to within $\pm 1 \cdot 10^{-4} \cdot w$ of the desired value, and its uncertainty is estimated to be no worse than $\pm 5 \cdot 10^{-4} \cdot w$. Conversion to mol fraction x was based on the molar masses of 44.010 $\text{g} \cdot \text{mol}^{-1}$ for CO_2 and 70.019 $\text{g} \cdot \text{mol}^{-1}$ for CHF_3. Afterwards, the supply vessel

was attached to the volumometer, which was evacuated to a pressure around 0.5 mPa, and the sample was expanded into the volumometer from the supply vessel.

After thermodynamic equilibrium of the sample in a homogeneous phase at a prescribed temperature and pressure was confirmed, temperature, pressure, and bellows position were measured and the sample density ρ_0 in the whole volume of the (volumometer + connecting lines + supply vessel) was calculated. Then, the connecting valve between the volumometer and the supply vessel was closed. After the sample in the volumometer reached thermodynamic equilibrium at the same temperature and pressure as that before the valve was closed, the bellows position was measured for calculating the inner volume V_i of the volumometer. The mass m of the sample confined in the volumometer was calculated as the product of ρ_0 and V_i with an uncertainty of $\pm 3{\cdot}10^{-4}{\cdot}m$. Then, the (p,ρ,T) measurements for the sample of mass m confined in the volumometer were carried out at various densities along given isotherms with the observation of the meniscus through the windows of the optical cell. It was possible to set the density ρ of the sample at the desired value to within $\pm 6{\cdot}10^{-4}{\cdot}\rho$, and its uncertainty was estimated to be no worse than $\pm 1{\cdot}10^{-3}{\cdot}\rho$.

The critical point of fluids and fluid mixtures can be determined by visual observation as the state where the critical opalescence is observed most intensely and equally both at the liquid phase and at the coexisting vapour phase with disappearance and reappearance of the vapour–liquid interface. The observation of

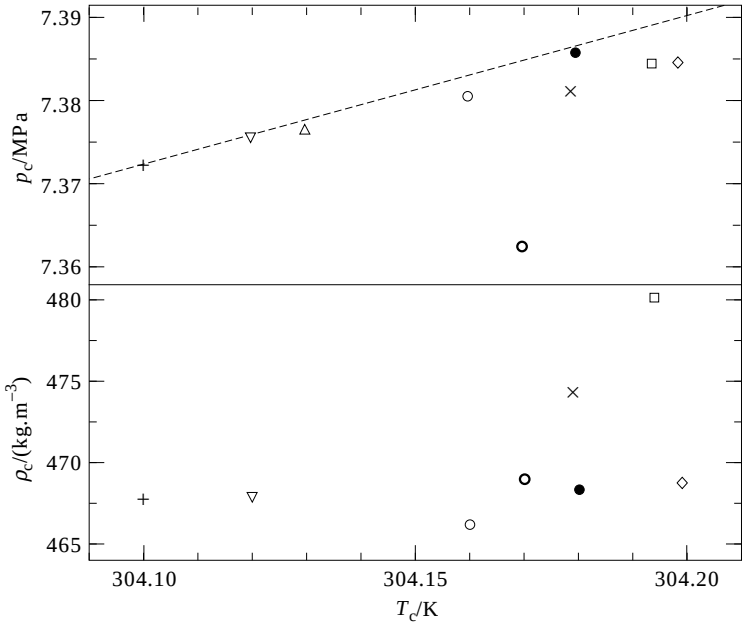

FIGURE 5. Comparison of the critical parameters for pure CO_2 with the literature values. ●, present work; △, Meyers and van Dusen;[4] ○, Michels *et al.*;[5] **O**, Cook;[6] ×, □, Wentrof;[7] ▽, Moldover;[8] ◇, Morrison;[9] +, Albright *et al.*;[10] – – –, vapour pressure calculated from the correlation by Duschek *et al.*[3]

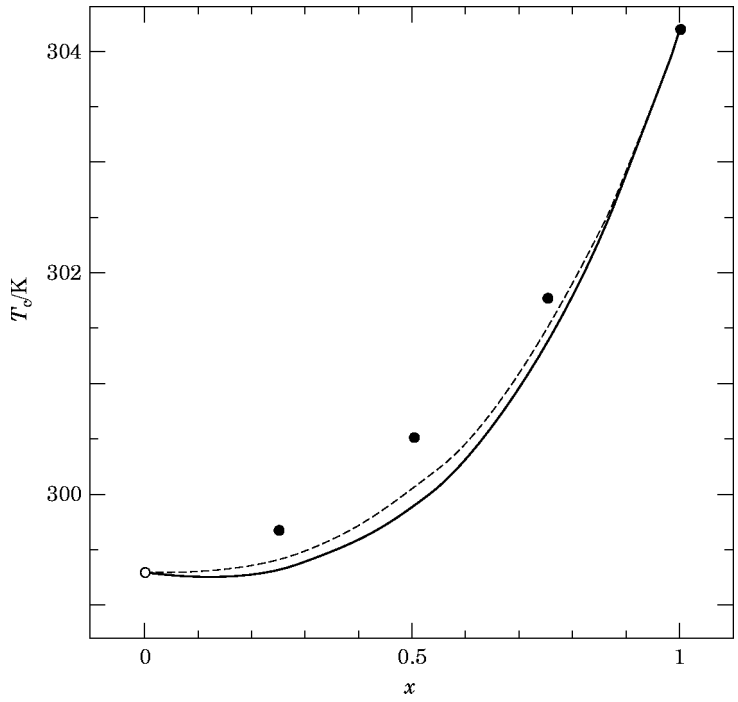

FIGURE 6. Composition dependence of the critical temperature T_c for $\{xCO_2 + (1-x)CHF_3\}$. ●, present work; ○, Ohgaki *et al*.;[11] ——, predicted by Peng–Robinson equation of state;[12] – – –, predicted by Soave–Redlich–Kwong equation of state.[13]

the meniscus for a sample of a given composition was started at a temperature where the vapour–liquid interface was observed, and continued as the temperature increased. At a temperature where the critical opalescence was observed, the temperature was kept constant, and the behaviour of the critical opalescence was observed carefully with variation of density. After adjusting the density to observe the critical opalescence most intensely at this temperature, the pressure was measured. The observation in the vicinity of the critical point was continued carefully for 12 h to 24 h keeping the temperature and density of the sample constant. This procedure was repeated, increasing and decreasing the temperature until the state where the critical opalescence was observed the most intensely among the temperatures and densities tried, was found. The temperature, density, and pressure measured at this state are considered to be the critical values. The density distribution as a function of the height of the sample due to the gravitational effect was not considered necessary to calculate the value of critical density.

The volume fraction purity of a sample of CO_2 supplied by Ekika Tansan Co., Ltd., was guaranteed to be 0.99999. The mass fraction purity of a sample of CHF_3 supplied by Asahi Glass Co., Ltd., was analysed as 0.999999 by the supplier. These pure samples were degassed three or four times by condensation with liquefied nitrogen.

3. Results

Measurements of the (p,ρ,T) properties and observations of the meniscus have been carried out in the critical region for pure CO_2 and $\{xCO_2 + (1 - x)CHF_3\}$ with $x = (0.7496, 0.5013, \text{and } 0.2522)$. The measurements for pure CO_2 have been carried out in order to illustrate the capability of the apparatus, and the results are given in table 1. The observations of the critical opalescence for $\{xCO_2 + (1 - x)CHF_3\}$ with $x = 0.2522$, as an example, are shown in figure 3 as a function of temperature and density in the range of temperatures: $-4.9\,\text{mK} \leq (T - T_c) \leq 15\,\text{mK}$, and of densities: $-1.9\,\text{kg·m}^{-3} \leq (\rho - \rho_c) \leq 2.1\,\text{kg·m}^{-3}$. Based on the results for observations of the critical opalescence, the critical parameters T_c, ρ_c, and p_c have been measured for mixtures of a given mole fraction and are given in table 2.

4. Discussion

The pressure values for pure CO_2 given in table 1 were compared with the values calculated by a correlation of the vapour pressure for pure CO_2 proposed by Duschek *et al.*[3] The deviations of the present results from the correlation are plotted in

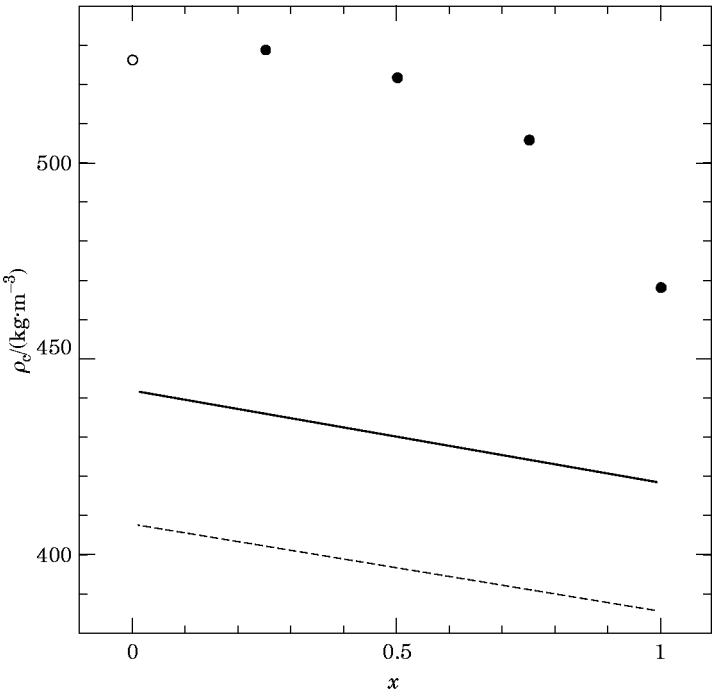

FIGURE 7. Composition dependence of the critical density ρ_c for $\{xCO_2 + (1 - x)CHF_3\}$. ●, present work; ○, Ohgaki *et al.*;[11] ——, predicted by Peng–Robinson equation of state;[12] – – –, predicted by Soave–Redlich–Kwong equation of state.[13]

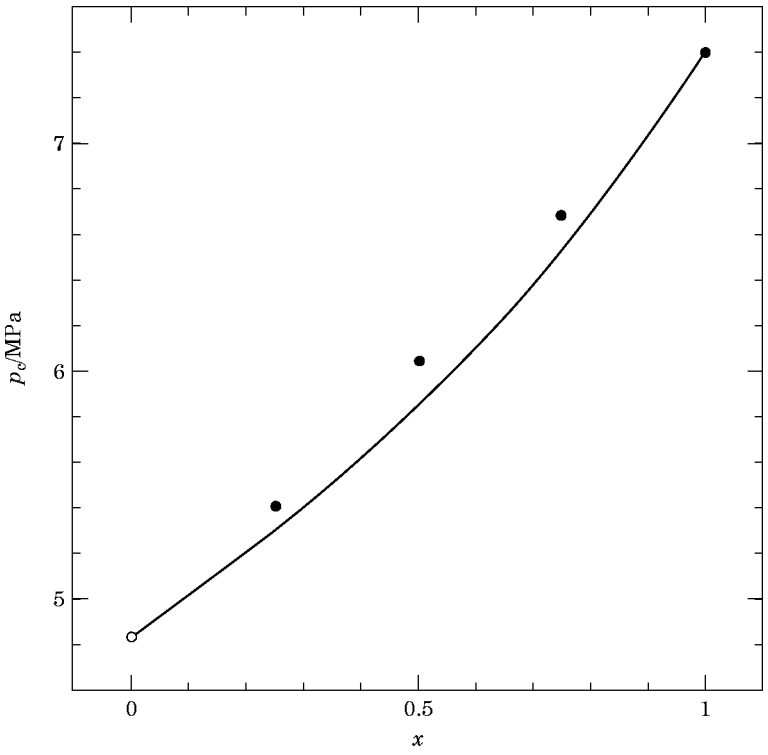

FIGURE 8. Composition dependence of the critical pressure p_c for $\{xCO_2 + (1 - x)CHF_3\}$. ●, present work; ○, Ohgaki *et al*.;[11] ——, predicted by Peng–Robinson equation of state.[12]

figure 4. Measurements whose temperatures are lower than $T_c = 304.129$ K of the correlation are systematically smaller than the calculated values by $3 \cdot 10^{-5} \cdot p$ to $1.5 \cdot 10^{-4} \cdot p$.

The critical parameters of the present measurements for pure CO_2 given in table 2 were compared with values given in the literature.[4–10] The critical properties in the literature and the present value are plotted in figure 5, where the vapour pressure curve and its extension to the higher temperatures calculated from the correlation by Duschek *et al*. are also plotted as a dashed curve as a function of temperature and pressure. In figure 5, the critical properties which are given for only T_c in the literature are not plotted. The present value of T_c is higher than that observed by Moldover[8] in 1974 by 0.06 K and lower than that observed by Morrison and Kincaid[9] in 1984 by 0.019 K. The present $\rho_c = (468 \pm 1)$ kg·m^{-3} agrees well with $\rho_c = 467.8$ kg·m^{-3} by Moldover and $\rho_c = 467.9$ kg·m^{-3} by Morrison and Kincaid. As for the difference of the critical pressure, the effect of vapour pressure due to the temperature difference should be considered. The differences of the present value of p_c from those reported by Moldover and Morrison and Kincaid are smaller than the uncertainty of ± 0.01 MPa in the present p_c measurement.

Composition dependence of the critical properties for $\{xCO_2 + (1 - x)CHF_3\}$ is shown in figures 6 to 8, where the critical properties as measured by Ohgaki *et al.*[11] for pure CHF_3 are plotted. The values predicted by the Peng–Robinson (PR) equation of state[12] and by the Soave–Redlich–Kwong (SRK) equation of state[13] are also depicted in figures 6 to 8 for comparison. The present critical temperatures are smaller than the mol-fraction-weighted means of the pure-component values by a maximum difference of $4 \cdot 10^{-3} \cdot T_c$. The predictions agree with each other and are smaller than the present values by $2 \cdot 10^{-3} \cdot T_c$. The present critical densities are larger than the mol-fraction-weighted means of the pure-component values by $0.03 \cdot \rho_c$ to $0.05 \cdot \rho_c$. The values predicted by the PR equation are smaller than the present values by about $0.2 \cdot \rho_c$ and those by the SRK equation are smaller than the present values by about $0.3 \cdot \rho_c$. These equations cannot predict the composition dependence of the critical densities. The present critical pressures are smaller than the mol-fraction-weighted means of the pure-component values by $1.1 \cdot 10^{-2} \cdot p_c$ to $1.3 \cdot 10^{-2} \cdot p_c$. The predictions agree with each other and are smaller than the present values by $0.03 \cdot p_c$.

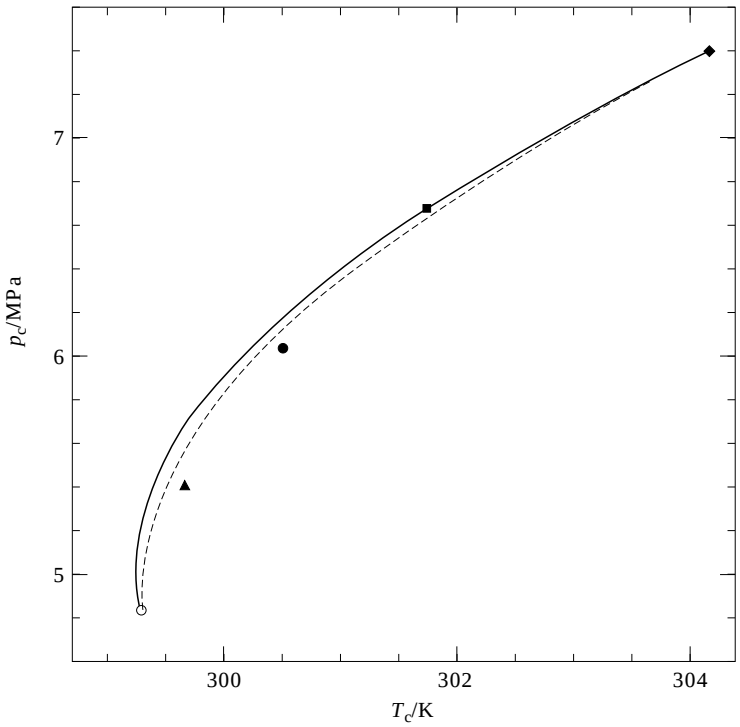

FIGURE 9. Critical pressure p_c against critical temperature T_c curve for $\{xCO_2 + (1 - x)CHF_3\}$. ◆, present work with $x = 1.0000$; ■, present work with $x = 0.7496$; ●, present work with $x = 0.5013$; ▲, present work with $x = 0.2522$; ○, Ohgaki *et al.*[11] with $x = 0.0000$; ——, predicted by Peng–Robinson equation of state;[12] – – –, predicted by Soave–Redlich–Kwong equation of state.[13]

Figure 9 shows the critical pressure against critical temperature curve for $\{xCO_2 + (1 - x)CHF_3\}$. In this figure the present critical properties, as well as the value measured by Ohgaki *et al*.,[11] for pure CHF_3 are plotted and the critical curves on the pressure against temperature plane predicted by the PR and SRK equations are also depicted for comparison. These equations represent well the critical curve of this system.

We are grateful to Professor E. U. Franck, University of Karlsruhe, F. R. G., for his valuable advice on the design of the apparatus. Y. Ando, K. Kasahara, and K. Shimoji have provided valuable assistance in the present work. The National Research Laboratory of Metrology, Tsukuba, kindly calibrated the platinum resistance thermometer. We were given the sample of CHF_3 by Asahi Glass Co. Ltd., Tokyo, who kindly analyzed the purity of the sample. The present work was supported through the Grant-in-Aid for Scientific Research Fund on Priority Areas (Supercritical Fluid 224) in 1992–1994 (Project No. 04238217, 05222220, 06214221) by the Ministry of Education, Science and Culture, Japan.

REFERENCES

1. Kabata, Y.; Yamaguchi, S.; Takada, M.; Uematsu, M. J. *Chem. Thermodynamics* **1992,** 24, 1019–1026.
2. Kabata, Y.; Yamaguchi, S.; Takada, M.; Uematsu, M. *J. Chem. Thermodynamics* **1992,** 24, 785–796.
3. Duschek, W.; Kleinrahm, R.; Wagner, W. J. *Chem. Thermodynamics* **1990,** 22, 841–864.
4. Meyers, C. H.; van Dusen, M. S. *J. Res. Natl. Bur. Stand. U.S.* **1933,** 10, 381–412.
5. Michels, A.; Blaisse, B.; Michels, C. *Proc. Roy. Soc.* **1937,** A160, 358–375.
6. Cook, D. *Proc. Roy. Soc.* **1953,** A219, 245–256.
7. Wentrof, R. H., Jr. *J. Chem. Phys.* **1956,** 24, 607–615.
8. Moldover, M. R. *J. Chem. Phys.* **1974,** 61, 1766–1778.
9. Morrison, G.; Kincaid, J. M. *AIChE J.* **1984,** 30, 257–262.
10. Albright, P. C.; Edwards, T. J.; Chen, Z. Y.; Sengers, J. V. *J. Chem. Phys.* **1987,** 87, 1717–1725.
11. Ohgaki, K.; Umezono, S.; Katayama, T. *J. Supercritical Fluid* **1990,** 3, 78–84.
12. Peng, D.-Y.; Robinson, D. B. *AIChE. J.* **1977,** 23, 137–144.
13. Soave, G. *Chem. Eng. Sci.* **1972,** 27, 1197–1203.

(Received 20 February 1996; in final form 19 April 1996)

WA-009/96